Theory of a Traveling-Wave Optical Maser*

FREDERICK ARONOWITZ
Military Products Group Research Department, Honeywell, Inc., Saint Paul, Minnesota
(Received 10 December 1964; revised manuscript received 5 March 1965)

A formal treatment of a traveling-wave optical maser is presented in which an assumed electromagnetic field in a rotating cavity, obeying Maxwell's equations, nonlinearly polarizes the moving gaseous atoms. The interaction is treated quantum mechanically in the frame of the moving atom. The resultant polarization, statistically summed over all velocity ensembles, is used as a source term in Maxwell's equations. The self-consistency gives a set of equations which determine the amplitudes and frequencies of oscillation of the modes of the independent oppositely directed traveling waves in terms of the parameters of the system. The results reduce to those obtained by Lamb for the case of a standing-wave optical maser with a stationary cavity. In addition, stability conditions on the oppositely directed waves are obtained for the cases where the active medium is a single isotope and a mixture of two isotopes.

1. INTRODUCTION

IN a past paper,[1] Lamb derived a technique for describing the operation of a multimode gaseous optical maser.[2,3] He considered a semiclassical model, in which the electromagnetic field obeyed Maxwell's equations while the gaseous atoms obeyed the laws of quantum mechanics. The treatment was a self-consistent one, in which an assumed electromagnetic field (standing wave) in the cavity polarized (nonlinearly) the moving gaseous atoms. The macroscopic polarization was then considered as a source term in Maxwell's equations. The derived field was equal to the original assumed field in the cavity. The self-consistency gave conditions on the amplitude of the field and the frequency of oscillation. The latter equations gave conditions on threshold, output power as a function of cavity tuning ("Lamb Dip"), frequency pulling and pushing, combination tones and the related phenomena of frequency locking.

The nonlinear contribution to the polarization arose from a third-order perturbation term in which the atomic system was considered to have interacted three times with the radiation field. Each interaction involved a Doppler phase shift such that at the time of observation the net phase shift was zero. The standing wave was considered to have been decomposed into two traveling waves and the atomic system interacted with the traveling waves, twice with the one going in one direction and once with the one going in the other direction. Since the empty-cavity normal modes were chosen to be standing waves, a standing-wave-type radiation field was necessary to obtain the correct contribution to the third-order polarization.

In the traveling-wave ring optical maser[4] (TWOM), where the waves running in each direction are independent, one cannot use Lamb's standing-wave formulation.

What will be presented in this paper is a modification of Lamb's formalism to allow treatment of both the traveling and the standing-wave optical maser (SWOM). The results agree with those obtained by Lamb for the SWOM case. For the TWOM, one obtains, in addition to the expected type of phenomena obtained by Lamb, conditions on the stability of the two independent counter-rotating beams. Taking for example, the single-longitudinal[5] mode case; it is shown that, on a rotating frame and for a single isotope, as the oscillations are tuned across the Doppler linewidth of the atomic transition, one of the two independent beams is extinguished. The beam that is extinguished depends on the sense of rotation and the direction of tuning. It is also shown that the presence of a small amount of an additional isotope maintains stability for both oscillations.[6] Equations are developed which give the relative intensity of each beam and the bandwidth of the unstable region.

2. MODIFICATION OF THE LAMB MODEL

As in the Lamb model, a self-consistent approach is used. An electromagnetic field is assumed to exist in the cavity. The interaction of the radiation with the ensemble of atoms having axial velocity components within an incremental velocity around velocity v is considered. This ensemble sees a Lorentz-transformed radiation field in its stationary frame. Thus the interaction between the cavity radiation field and the moving atoms is reduced to an interaction between a Doppler-shifted radiation field and an ensemble of stationary atoms. In the Lorentz transformation, amplitude transformations are neglected. Only frequency transformations are considered.

In the frame of the moving atoms, the radiation field polarizes the atoms. By application of the inverse

* To be submitted in partial fulfillment of the requirements of the degree of Doctor of Philosophy at New York University.
[1] W. E. Lamb, Jr., Phys. Rev. 134, A1429 (1964).
[2] A. L. Schawlow and C. H. Townes, Phys. Rev. 112, 1940 (1958).
[3] A. Javan, W. R. Bennett, Jr., and D. R. Herriott, Phys. Rev. Letters 6, 106 (1961).
[4] W. M. Macek and D. T. M. Davis, Jr., Appl. Phys. Letters 2, 67 (1963).
[5] A. G. Fox and T. Li, Bell System Tech. J. 40, 61 (1961).
[6] The possibility of this occurring was suggested by J. E. Killpatrick (private communication).

Lorentz transformation, the polarization is transformed back to the cavity frame. The polarization in the cavity frame is then averaged over all velocity ensembles. The macroscopic polarization is then used as a source term in Maxwell's equations to calculate a reaction field. For self-consistency the calculated reaction field must equal the original assumed radiation field in the cavity. This self-consistency gives a condition on the amplitudes and frequencies of the modes of the radiation field.

3. ELECTROMAGNETIC FIELD EQUATIONS

From Maxwell's equations the electric field in the nonrotating cavity is obtained from the approximate wave equation (mks):

$$\frac{\partial^2 E}{\partial z^2}-\epsilon_0\mu_0\frac{\omega}{Q}\frac{\partial E}{\partial t}-\epsilon_0\mu_0\frac{\partial^2 E}{\partial t^2}=-\mu_0\omega^2 P. \tag{1}$$

In Eq. (1) only the axial variation of E has been considered. The passive Q of the system has been obtained from the fictional conductivity as

$$Q=\epsilon_0\omega/\sigma. \tag{2}$$

Since the macroscopic polarization is nearly monochromatic, the second time derivative of P has been replaced by $-\omega^2 P$. Consistent with the approximation of considering only frequency changes arising from Lorentz transformations, magnetization terms have been neglected in the source term in Eq. (1).

For the case of an empty lossless cavity containing two oppositely directed traveling waves, the solution of Eq. (1) gives

$$E(z,t)=E_1\sin(Kz+\Omega t)+E_2\sin(Kz-\Omega t)\,. \tag{3}$$

This leads one to expand the solution of Eq. (1) into the set of empty-cavity normal-mode eigenfunctions (ECNME)

$$E(z,t)=\sum_n\left[A_n(t)U_n(z)+\tilde{A}_n(t)V_n(z)\right], \tag{4}$$

with

$$U_n(z)=\sin K_n z, \tag{5}$$

$$V_n(z)=\cos K_n z. \tag{6}$$

For a ring cavity of length L, the function $E(z,t)$ satisfies periodic boundary conditions, giving the wave number

$$K_n=2\pi n/L. \tag{7}$$

The ECNME satisfy the equation

$$\left[\frac{d^2}{dz^2}+\epsilon_0\mu_0\Omega_n^2\right]\begin{pmatrix}U_n(z)\\V_n(z)\end{pmatrix}=0. \tag{8}$$

Making use of the orthogonality properties of the ECNME, Eqs. (1), (4), and (8) give the following set of equations:

$$\left[\frac{d^2}{dz^2}+\frac{\omega}{Q_n}\frac{d}{dt}+\Omega_n^2\right]\begin{pmatrix}A_n(t)\\\tilde{A}_n(t)\end{pmatrix}=\frac{\omega^2}{\epsilon_0}\begin{pmatrix}P_n(t)\\\tilde{P}_n(t)\end{pmatrix}, \tag{9}$$

with

$$P_n(t)=(2/L)\int_0^L P(z,t)U_n(z)dz, \tag{10}$$

$$\tilde{P}_n(t)=(2/L)\int_0^L P(z,t)V_n(z)dz. \tag{11}$$

In Eq. (9) the Q of each mode has been subscripted for greater generality.

As discussed by Lamb, for the case of the principal mode separation being much greater than the passive cavity width such that time-dependent Fourier components of A_n and P_n which are far removed from the cavity resonance can be neglected, one can write

$$A_n(t)=E_{1n}(t)\cos[\omega_{1n}t+\Phi_{1n}(t)]+E_{2n}(t)\cos[\omega_{2n}t+\Phi_{2n}(t)], \tag{12}$$

$$\tilde{A}_n(t)=E_{1n}(t)\sin[\omega_{1n}t+\Phi_{1n}(t)]-E_{2n}(t)\sin[\omega_{2n}t+\Phi_{2n}(t)], \tag{13}$$

$$P_n(t)=S_{1n}(t)\sin[\omega_{1n}t+\Phi_{1n}(t)]+C_{1n}(t)\cos[\omega_{1n}t+\Phi_{1n}(t)], \tag{14}$$

$$\tilde{P}_n(t)=\tilde{S}_{1n}(t)\sin[\omega_{1n}t+\Phi_{1n}(t)]+\tilde{C}_{1n}(t)\cos[\omega_{1n}t+\Phi_{1n}(t)]. \tag{15}$$

In Eqs. (12)–(15) the time-dependent coefficients are slowly varying with respect to optical frequencies. The form of Eqs. (12) and (13) is such as to reduce, in an empty cavity, to two oppositely directed traveling waves.

Substituting Eqs. (12)–(15) into Eq. (9) and equating coefficients of $\sin[\omega_{1n}t+\Phi_{1n}]$ and $\cos[\omega_{1n}t+\Phi_{1n}]$ to zero, self-consistency equations are found as

$$\dot{E}_{1n}+\tfrac{1}{2}(\omega/Q_n)E_{1n}=-\tfrac{1}{4}(\omega/\epsilon_0)[S_{1n}-\tilde{C}_{1n}], \tag{16}$$

$$(\Omega_{1n}-\omega_{1n}-\dot{\Phi}_{1n})E_{1n}=\tfrac{1}{4}(\omega/\epsilon_0)[C_{1n}+\tilde{S}_{1n}], \tag{17}$$

$$\dot{E}_{2n}+\tfrac{1}{2}(\omega/Q_n)E_{2n}=-\tfrac{1}{4}(\omega/\epsilon_0)[(S_{1n}+\tilde{C}_{1n})\cos\psi_n+(C_{1n}-\tilde{S}_{1n})\sin\psi_n], \tag{18}$$

$$(\Omega_{2n}-\omega_{2n}-\dot{\Phi}_{2n})E_{2n}=-\tfrac{1}{4}(\omega/\epsilon_0)[(S_{1n}+\tilde{C}_{1n})\sin\psi_n-(C_{1n}-\tilde{S}_{1n})\cos\psi_n], \tag{19}$$

where

$$\psi_n=(\omega_{2n}-\omega_{1n})t+\Phi_{2n}(t)-\Phi_{1n}(t) \tag{20}$$

is a slowly varying function of time. In Eqs. (16)–(19), second derivatives of the amplitudes have been neglected, as well as relative terms of Q_n^{-1}.

To allow for the description of a cavity located on a rotating frame, which is of course the usual case for an experiment on the surface of the earth, the ECNME

frequencies have been subscripted for the oppositely directed waves.[7]

4. POLARIZATION OF THE MEDIUM

This section closely parallels the corresponding section in Lamb's paper[1] in basic format.

Consider an ideal two-excited-level system. Atoms are excited to either of levels a or b (Energy $\hbar W_a > \hbar W_b$) at some time t_0. The atom can decay spontaneously at rate γ_a, γ_b, respectively, or, owing to the presence of the radiation field, undergo a stimulated transition. For oscillation to occur, it is assumed that a population inversion exists. Expanding the state of the atomic system in terms of the unperturbed set of states of the atom, here taken as only levels a and b, the equation of motion for the expansion coefficients is[1,8]

$$\dot{\rho} = -i[H,\rho] - \tfrac{1}{2}(\Gamma\rho + \rho\Gamma) , \tag{21}$$

where

$$\rho = \begin{pmatrix} aa^* & ab^* \\ ba^* & bb^* \end{pmatrix} = \begin{pmatrix} \rho_{aa} & \rho_{ab} \\ \rho_{ba} & \rho_{bb} \end{pmatrix}, \tag{22}$$

$$H = \begin{pmatrix} W_a & V_{ab}(t) \\ V_{ba}(t) & W_b \end{pmatrix}, \quad \Gamma = \begin{pmatrix} \gamma_a & 0 \\ 0 & \gamma_b \end{pmatrix}. \tag{23}$$

The matrix element between states a and b of the interaction is given as

$$hV_{ab}(t) = -\mu_{ab}E(z,v,t) , \tag{24}$$

where μ_{ab} is the matrix element of the electric dipole moment taken between states a and b and $E(z,v,t)$ is the electric field as seen by the atom. It is this point in which the formalism differs from that as presented by Lamb.[1] Since the atom is described in its own Lorentz frame, the atom always remains at the point where it was excited. Collisions are neglected. Thus ρ is characterized by the following parameters: t_0 and z, defined in the moving frame; v, the axial velocity components of the atom with respect to the cavity; $\alpha = a,b$, the state to which the atom was initially excited at time t_0; t, the time at which we wish to observe the system. Since the atoms are of thermal velocity, simple Calilean transformations are used so that atom time is simultaneous with cavity time and atoms in all frames see the same cavity length. The ρ which describes the total ensemble of atoms excited to either state at position z, having velocity component v is written as

$$\rho(z,v,t) = \sum_{\alpha=a,b} \int dz_0 \int_{-\infty}^{t} dt_0 \lambda_\alpha(t_0,z,v)\rho(\alpha,t_0,z,v,t)\delta(z-z_0) , \tag{25}$$

where $\lambda_\alpha(t_0,z,v)$ is the rate per unit volume of exciting atoms having velocity component v, to state α at position z, at time t_0. Equation (25) contains a trivial integration containing a delta function over all the initial excitation points for the velocity ensemble. This occurs because the interaction is treated in the stationary atom frame.

The cavity field as given by Eqs. (4), (12), and (13) is seen by an atom at time t and at position z in a moving frame as

$$\begin{aligned} E(z,v,t) = \sum_n \big(&\{E_{1n}\cos[\omega_{1n}(1+v/c)t+\Phi_{1n}] \\ &+ E_{2n}\cos[\omega_{2n}(1-v/c)t+\Phi_{2n}]\} U_n(z) \\ &+ \{E_{1n}\sin[\omega_{1n}(1+v/c)t+\Phi_{1n}] \\ &- E_{2n}\sin[\omega_{2n}(1-v/c)t+\Phi_{2n}]\} V_n(z)\big) . \end{aligned} \tag{26}$$

The coordinate system has been chosen as to arbitrarily cause the velocity ensemble to see the traveling wave E_{1n} and E_{2n} as being Doppler-shifted up and down, respectively. The K_n in the ECNME are still given by Eq. (7) as $2\pi n/L$.

The contribution to the polarization by the moving atoms at position z is

$$P(z,v,t) = \mu_{ba}\rho_{ab}(z,v,t) + \text{c.c.} . \tag{27}$$

The Fourier components of the polarization due to all the atoms in the velocity ensemble located at point z is

$$P_n(v,t) = (2/L)\int_0^L P(z,v,t)U_n(z)dz , \tag{28}$$

$$\tilde{P}_n(v,t) = (2/L)\int_0^L P(z,v,t)V_n(z)dz . \tag{29}$$

The macroscopic Fourier components of the polarization are obtained by transforming $P_n(v,t)$ and $\tilde{P}_n(v,t)$ back to the cavity frame and averaging over all velocities. In performing the transformation it is first necessary to group $P(z,v,t)$ into terms having the form of oppositely directed traveling waves. The terms will be of the form $\exp i[\pm Kz - \omega_{1n}(1\mp v/c)t - \Phi_{1n}]$. Thus to make the inverse Lorentz transformation, it is sufficient to multiply each term by $\exp(\mp i\omega_{1n}tv/c)$, respectively. This will be more clearly shown in what follows.

5. CALCULATION OF POLARIZATION FOR SINGLE MODE

The solution of Eq. (21) for $\rho(\alpha,t_0,z,v,t)$ is obtained by treating the interaction between the radiation field and the atomic system as a perturbation and expanding $\rho(\alpha,t_0,z,v,t)$ in orders of the interaction. This has been done by Lamb[1] and will not be repeated here.

For a single mode the interaction is obtained from

[7] This has been shown by C. V. Heer, Phys. Rev. **134**, A799 (1964). Refer to Appendix I for a formal derivation using the traveling-wave formalism as presented in this paper.

[8] W. E. Lamb, Jr., and T. M. Sanders, Jr., Phys. Rev. **119**, 1901 (1960).

Eqs. (24) and (26) as

$$V_{ab}(t)=-(\mu_{ab}/\hbar)[[E_1\cos((\omega_1+Kv)t+\Phi_1)+E_2\cos((\omega_2-Kv)t+\Phi_2)]U_n(z)+[E_1\sin((\omega_1+Kv)t+\Phi_1)-E_2\sin((\omega_2-Kv)t+\Phi_2)]V_n(z)]. \quad (30)$$

In Eq. (30) the distinction between the ECNME and oscillating wave number has been neglected. The mode subscript on the amplitudes has also been dropped. Calculating the first-order polarization by evaluating the integrals in somewhat the same manner as prescribed by Lamb[1] (details are to be found in Appendix II), the conditions on the amplitudes and frequencies of oscillation of the oppositely directed traveling waves are found as

$$\dot{E}_i+\tfrac{1}{2}(\omega/Q_i)E_i=\tfrac{1}{2}(\omega/\epsilon_0)\pi^{1/2}AE_i\exp-\xi_i^2, \quad (31)$$

$$\omega_i=\Omega_i-(\omega/\epsilon_0)AF(\xi_i), \quad i=1,2, \quad (32)$$

where

$$F(\xi_i)=\exp(-\xi_i^2)\int_0^{\xi_i}dx\exp x^2, \quad (33)$$

$$A=|\mu_{ab}|^2\bar{N}(t)/(\hbar Ku), \quad (34)$$

$$\xi_i=(\omega_i-\omega)/(Ku). \quad (35)$$

In writing Eqs. (31) and (32), it has been assumed that the Doppler width

$$\Delta\omega=2(\ln 2)^{1/2}Ku,$$

is much larger than the natural width. In Eq. (34), $\bar{N}(t)$ is the average excitation inversion density.

Equations (31) and (32) are the standard threshold conditions for independent oscillation. For the case of a SWOM, Eqs. (31) and (32) reduce to those obtained by Lamb.[1]

6. POPULATION INVERSION

A second-order perturbation expansion gives the average population inversion of a given velocity ensemble as (details are in Appendix III)

$$\Delta\rho(v,t)=\bar{N}(t)W(v)\times[1-2I_1\mathfrak{L}(\xi_1+v/u)-2I_2\mathfrak{L}(\xi_2-v/u)], \quad (36)$$

where $W(v)$ is the normalized velocity distribution.

The dimensionless intensity of each beam is

$$I_i=|\mu_{ab}|^2E_i^2/(2\hbar^2\gamma_a\gamma_b). \quad (37)$$

The Lorentzian function $\mathfrak{L}(\xi)$ is defined as

$$\mathfrak{L}(\xi)=[1+(\xi/\eta)^2]^{-1}, \quad (38)$$

where η is the ratio of the natural to Doppler width, or

$$\eta=\gamma_{ab}/Ku=\tfrac{1}{2}\Delta\omega_n/(Ku). \quad (39)$$

Equation (36) shows the saturating effects of the oscillations on the unsaturated population inversion. A plot of average population inversion versus velocity ensemble shows the Gaussian velocity distribution with two Lorentzian holes "burnt" into the curve. This can better be seen by writing Eq. (36) in the non-normalized form

$$\Delta\rho(v,t)=\bar{N}(t)W(v)\left\{1-2I_1\left[1+\left(\frac{\omega-\omega_1-Kv}{\frac{1}{2}\Delta\omega_n}\right)^2\right]^{-1}-2I_2\left[1+\left(\frac{\omega-\omega_1-\Delta\Omega+Kv}{\frac{1}{2}\Delta\omega_n}\right)^2\right]^{-1}\right\}. \quad (40)$$

In Eq. (40) pulling effects have been neglected and for a first approximation $\Delta\Omega=\omega_2-\omega_1$. Thus, the depth of each hole is determined by the intensity traveling in each direction and the width is equal to the natural width of the atomic transition. For the case when

$$0<\Delta\Omega\ll\omega-\omega_1,$$

the holes are located on opposite sides of the inversion curve. As the oscillations are tuned through the center of the atomic transition such that $\Delta\Omega=\omega-\omega_1$ one of the holes is found to be symmetrically placed on the inversion curve. As this point is passed it is found that both holes are centered on the same side of the inversion curve. It is in this region that strong mode-competition effects are expected, although mode-competition effects are present at any point of oscillation. Mode competition is at a maximum when the two holes completely overlap, which occurs when $\Delta\Omega=2(\omega-\omega_1)$. At this point the two oscillation frequencies ω_1 and ω_2 are symmetrically located about the atomic transition frequency ω.

At first sight it is not even obvious that two independent oppositely directed traveling waves can exist at any frequency. This question will be considered after the calculation of the third-order Fourier component of polarization, which will allow calculation of the intensities I_1 and I_2.

It should also be noted that Eq. (40) gives the validity condition on the strength of the field such that convergence of the perturbation expansion occurs. Physically it says that the relative depth of the hole burnt into the inversion curve is small, or I_1, $I_2\ll 1$.

It should also be noted that Eq. (40) is what would be calculated using Lamb's formalism for the case of a SWOM if $\Delta\Omega=0$ and

$$(I_1=I_2)_{\text{TWOM}}=\tfrac{1}{4}I_{\text{SWOM}}. \quad (41)$$

7. THIRD-ORDER POLARIZATION

The expression for, and the details of the calculation of the third-order Fourier components of the polarization are found in Appendix IV. The expression is similar to that as derived by Lamb,[1] except for the Lorentzian operator necessary to transform the polarization contribution of a single velocity ensemble from the moving atom frame to the cavity frame.

In the "Doppler limit" the self-consistent equations can be approximated as

$$\dot{E}_1+\tfrac{1}{2}(\omega/Q_1)E_1=\tfrac{1}{2}(\omega/\epsilon_0)\pi^{1/2}AE_1 \times[Z_i(\xi_1)/Z_i(0)-I_1\exp(-\xi_1^2) -I_2\exp(-\xi_1^2)\mathfrak{L}(\xi)], \quad (42)$$

$$\dot{E}_2+\tfrac{1}{2}(\omega/Q_2)E_2=\tfrac{1}{2}(\omega/\epsilon_0)\pi^{1/2}AE_2 \times[Z_i(\xi_2)/Z_i(0)-I_2\exp(-\xi_2^2) -I_1\exp(-\xi_1^2)\mathfrak{L}(\xi)], \quad (43)$$

$$(\omega_1+\dot{\Phi}_1-\Omega_1)=\tfrac{1}{2}(\omega/\epsilon_0)A \times[Z_r(\xi_1)+I_2(\xi/\eta)\mathfrak{L}(\xi)Z_i(\xi_2)], \quad (44)$$

$$\omega_2+\dot{\Phi}_2-\Omega_2=\tfrac{1}{2}(\omega/\epsilon_0)A \times[Z_r(\xi_2)+I_1(\xi/\eta)\mathfrak{L}(\xi)Z_i(\xi_1)], \quad (45)$$

where Z_r and Z_i are the real and imaginary parts of the "plasma dispersion function," as defined in Appendix II.

For the case of a SWOM, Eqs. (42)–(45) reduce to those derived by Lamb, except for the added exponential factor $\exp(-\xi_i^2)$ next to each dimensionless intensity factor I_i. As shown in Appendix IV, the exponential factor arises from the evaluation of the integrals without the delta-function approximation. The physical significance in being able to insert or omit the exponential factor arises in the criteria for the validity of the perturbation expansion. The exponential factor becomes significant for large ξ_i, or for operation "away" from the center frequency of the atomic transition. This implies a gain/loss value such that as the oscillation frequency is tuned through the Doppler center, the depth of the hole will be great enough such as to invalidate the perturbation expansion. Hence, the solution is expected to be most valid in the region where the exponential differs little from unity. However, when the effect of multiple isotopes upon the operation of the system is considered it will be essential to keep the exponential factor.

From a study of the form of the interaction which leads to Eq. (IV.3), it is seen that the dominant contribution to the polarization occurs when the accumulated Doppler phase shift cancels. This corresponds to the case of pure inhomogeneous broadening and the third order contribution to Eqs. (42)–(45) contain only this dominant part of the interaction. The third-order polarization occurs due to the atom undergoing three stimulated interactions with the net radiation field at times $t'''<t''<t'$. The choice of the traveling wave with which the atom interacts is not arbitrary. From the form of Eqs. (IV.3) and (IV.4) it is seen that for the dominant contribution to the polarization, the atom's first two interactions are with the same traveling wave, while the third interaction may be with either of the two traveling waves. This order of interaction also applies for the case of a SWOM.

From the case of broadening somewhat between pure inhomogeneous and pure homogeneous, contributions to the polarization can occur when the accumulated Doppler phase shifts are not zero. Some of these contributions have been evaluated in Appendix IV, although they have not been included in the self-consistent equations (42)–(45), and have been shown to be of higher order in the parameter (natural width/Doppler width).

8. STABILITY FOR SINGLE ISOTOPE

At steady state, Eqs. (42) and (43) give two simultaneous equations for the dimensionless intensities I_1 and I_2, which can be solved to give

$$I_1=\exp(\xi_1^2)[H(\xi_1)-\mathfrak{L}(\xi)H(\xi_2)][1-\mathfrak{L}^2(\xi)]^{-1}, \quad (46)$$

$$I_2=\exp(\xi_2^2)[H(\xi_2)-\mathfrak{L}(\xi)H(\xi_1)][1-\mathfrak{L}^2(\xi)]^{-1}, \quad (47)$$

where

$$H(\xi_i)=Z_i(\xi_i)/Z_i(0)-\mathfrak{N}_i^{-1}, \quad i=1,2, \quad (48)$$

and $\mathfrak{N}_i$ is the ratio of the excitation inversion density to the threshold value of the excitation inversion density taken for oscillations at the center frequency of the atomic transition. Thus $H(\xi_i)$ is proportional to the depth of the hole produced by the radiation ξ_i. Since $\mathfrak{L}(\xi)$ approaches unity as ξ approaches zero, Eqs. (46) and (47) contain a singularity. But, depending on the direction of tuning, one of the numerators of Eqs. (46) and (47) goes to zero before the average of the oscillating frequencies passes through the center of the atomic transition. At this point, one of the two oppositely traveling waves is extinguished and this determines the range of validity of Eqs. (46) and (47). For example, consider the case of tuning in the direction of increasing frequencies. Before the oscillation frequency is tuned through the Doppler center and for the case of losses for radiation traveling in either direction being equal, $H(\xi_2)$ is just slightly greater than $H(\xi_1)$. Then, from Eq. (46) the radiation oscillating at ξ_1 will extinguish. If the oscillation frequency were to be tuned in the direction of decreasing frequencies, it would again be the radiation oscillating farthest from the Doppler center (I_2 in this case) which would extinguish. It is interesting to note that if the direction of rotation of the rotating frame were reversed (perform the experiment in the southern hemisphere) the traveling wave that would be extinguished as we tuned through the Doppler curve would be the opposite of the one that was previously found to be extinguished.

A calculation giving the point where one of the modes is extinguished gives

$$|\xi/\Delta\xi|\approx(4\ln 2)(\Delta\omega_n/\Delta\omega)^2\mathfrak{N}/(\mathfrak{N}-1), \quad (49)$$

where

$$\Delta\xi=\tfrac{1}{2}(\xi_2-\xi_1). \quad (50)$$

For the Ne 1.15-micron transition and for a gain/loss ratio of 2,

$$\xi=0.02\Delta\xi. \quad (51)$$

Thus both the oppositely traveling waves can oscillate

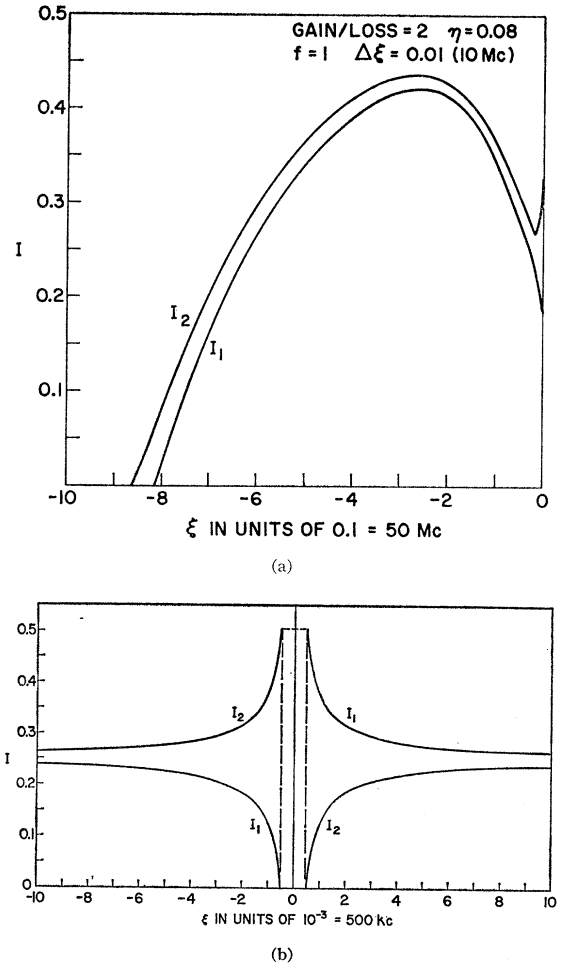

FIG. 1. Plot of intensities of oppositely directed traveling waves versus tuning of degenerate cavity frequency through single-isotope Doppler-gain curve. In Fig. (a) the intensities are symmetric about the Doppler center with the role of I_1 and I_2 interchanged. Figure (b) is a blowup of the center region. The separation between the curves of Fig. (a) has been exaggerated.

until the holes are almost completely overlapped. A plot of I_1 and I_2 as the frequency of oscillation is tuned through the atomic transition gain curve is shown in Figs. 1(a) and 1(b). A splitting of $\Delta\xi=0.01$ (10 Mc/sec) has been chosen for the ECNME frequencies. For high values of $|\xi|$, both modes are extinguished as they fall below threshold. As the oscillation frequencies are tuned through the center of the atomic transition, the roles of I_1 and I_2 are interchanged. As the tuning moves through the unstable region, the beam which does not extinguish (determined by the direction of tuning) will remain essentially constant and then quickly fall to zero as the other beam takes over. Then the intensities will follow the curves plotted in Figs. 1(a) and 1(b).

It should be emphasized that the consideration of the single isotope case is similar to discussing forced oscillations without damping. As will be shown in the next section, the presence of even a trace of an additional isotope will remove the singularity from the intensity equations.

9. STABILITY—TWO-ISOTOPE CASE

Consider the addition of a second isotope to the system such that the ratio of atoms of each type is $f/(1-f)$. Let primes signify quantities pertaining to be second isotope. Then the excitation inversion density for each velocity ensemble is

$$N(z,v,t)=fN(z,t)W(v)+(1-f)N(z,t)W'(v)\,. \quad (52)$$

In analogous fashion to the single-isotope case, the self-consistency amplitude equations, correct to the third order, are found to be

$$\dot{E}_1+\tfrac{1}{2}(\omega/Q_1)E_1=\tfrac{1}{2}(\omega/\epsilon_0)\pi^{1/2}AE_1 \times\{f[\exp(-\xi_1^2)-I_1\exp(-\xi_1^2) -I_2\exp(-\xi_2^2)\mathfrak{L}(\xi)] +(m'/m)^{1/2}(1-f)[\exp(-\xi_1'^2) -I_1\exp(-\xi_1'^2) -I_2\exp(-\xi_2'^2)\mathfrak{L}(\xi')]\}\,. \quad (53)$$

$$\dot{E}_2+\tfrac{1}{2}(\omega/Q_2)E_2=\tfrac{1}{2}(\omega/\epsilon_0)\pi^{1/2}AE_1 \times\{f[\exp(-\xi_2^2)-I_2\exp(-\xi_2^2) -I_1\exp(-\xi_1^2)\mathfrak{L}(\xi)] +(m'/m)^{1/2}(1-f)[\exp(-\xi_2'^2) -I_2\exp(-\xi_2'^2) -I_1\exp(-\xi_1'^2)\mathfrak{L}(\xi')]\}\,. \quad (54)$$

The ratio of the masses of the two isotopes arises from the difference in Doppler widths for each isotope. Comparing Eqs. (53) and (54) to the amplitude equations for the single isotope, it is seen that the equation could easily be generalized for any number of isotopes. Likewise, the frequency equations could be written by inspection of the equations for the single-isotope case. At steady state the intensity of both traveling waves is found from Eqs. (53) and (54) as

$$I_1=\text{Num./Den.}, \quad (55)$$

where

$$\text{Num.}=[f\exp(-\xi_1^2)+f'\exp(-\xi_1'^2)-\mathfrak{N}_1^{-1}] \times[f\exp-\xi_2^2+f'\exp-\xi_2'^2] -[f\exp(-\xi_2^2)+f'\exp(-\xi_2'^2)-\mathfrak{N}_2^{-1}] \times[f\exp(-\xi_2^2)\mathfrak{L}(\xi)+f'\exp(-\xi_2'^2)\mathfrak{L}(\xi')], \quad (56)$$

$$\text{Den.}=f^2\exp(-\xi_1^2-\xi_2^2)[1-\mathfrak{L}^2(\xi)] +f'^2\exp(-\xi_1'^2-\xi_2'^2)[1-\mathfrak{L}^2(\xi')] +ff'[1-\mathfrak{L}(\xi)\mathfrak{L}(\xi')] \times[\exp(-\xi_1^2-\xi_2'^2)+\exp(-\xi_1'^2-\xi_2^2)], \quad (57)$$

and

$$f'=(m'/m)^{1/2}(1-f)\,. \quad (58)$$

The intensity I_2 is obtained by interchanging the subscripts 1 and 2 in Eqs. (55)–(57).

Note that as mentioned, the two-isotope case differs

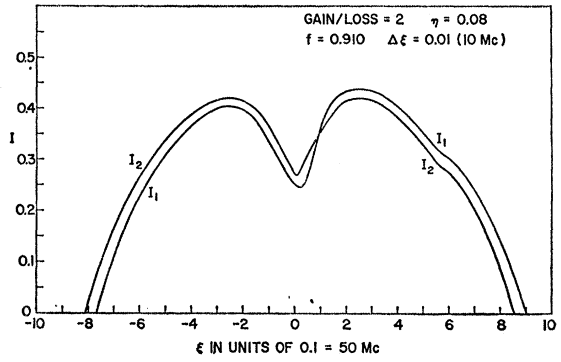

FIG. 2. Intensities versus tuning for natural neon.

from the single-isotope case that in Eq. (55) does not contain a singularity. Figure 2 shows a plot of intensity versus tuning for natural neon. The effects of Ne^{21} have been neglected. The separation of the transition of Ne^{22} has been taken as 260 Mc/sec.[9] The crossover point where the two intensities are equal is seen to have shifted approximately 40 Mc/sec above the center frequency of Ne^{20}. In addition, a slight bump in the curves is seen at the center frequency of Ne^{22}.

Figures 3(a), 3(b), and 3(c) show the effect of a trace of isotope Ne^{22} on the stability of both traveling modes. For a concentration of 99.9999% Ne^{20} it is seen that there exists a narrow gap where both beams are stable, inside the region of instability. Figure 3(b) shows the case of 99.99% Ne^{20}. It is seen that there is no region of instability and that the crossover point is starting to move to higher frequencies. In Fig. 3(c), for the case of 99.9% Ne^{20}, it is seen that there is essentially a smooth transition through the center of the Lamb dip.

The average population inversion as a function of velocity ensemble is obtained to second order as

$$\Delta\rho(v,t)=f\bar{N}(t)W(v)[1-2I_1\mathfrak{L}(\xi_1+v/u) -2I_2\mathfrak{L}(\xi_2-v/u)]+(1-f)\bar{N}(t)W'(v) \times[1-2I_1\mathfrak{L}(\xi_1'+v/u)-2I_2\mathfrak{L}(\xi_2'-v/u)]. \quad (59)$$

10. GENERAL DISCUSSION

For the single isotope, the population inversion curve versus velocity ensemble and the gain curve versus frequency are quite similar in shape (the hole width in the gain curve is twice, in comparable units, the hole width in the population inversion curve) and it is easy to confuse the meaning of each. For the two-isotope case, the curves are radically different. From Eq. (59) the population inversion curve is composed of two velocity-distribution functions, each located symmetrically about the $v=0$ axis. The two holes burnt into each curve are of different depth and are located at different distances from the $v=0$ axis. There is no significance to the superposition of the two curves.

[9] A. Szoke and A. Javan, Phys. Rev. Letters **10**, 521 (1963).

The gain curve is obtained from the right-hand sides of Eqs. (53) and (54), although strictly speaking the amplitude equations only give the condition that gain equals loss, at the frequency of oscillation. It is the interpretation of the equations that determines gain at a frequency other than the frequency of oscillation. In addition, for a TWOM located on a rotating frame, the gain profile versus frequency in the presence of oscillations at a fixed frequency is different for radiation

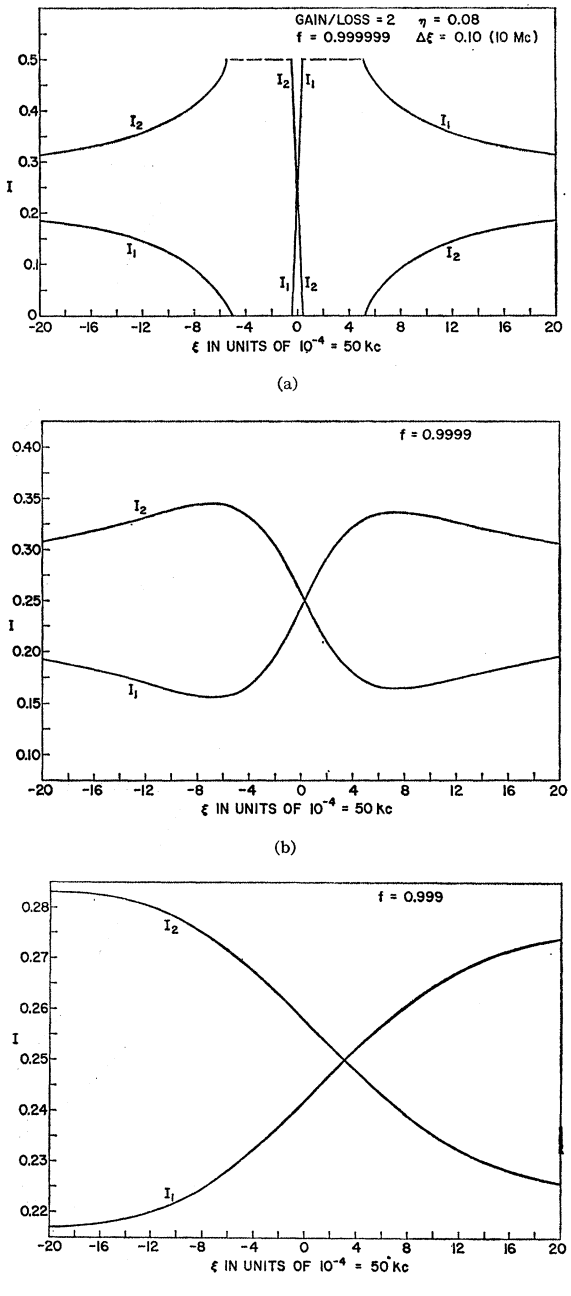

FIG. 3. Intensity versus tuning in region of Doppler center for Ne^{20} with an added trace of Ne^{22}.

traveling in different directions. As an illustration, consider the gain profile from the point of view of radiation traveling in the same direction as the radiation oscillating at $\omega_2<\omega$. (See Fig. 4(a).) Then at ω_2 there will be two holes, one in each of the single isotope Gaussian gain profiles. The holes due to the radiation oscillating at ω_1 will burn image holes at $-\xi_1$ and $-\xi_1'$, respectively. From the Lorentzian functions in Eqs. (53) and (54) it is seen that the width of the holes burnt into the gain curve is twice the width of the holes burnt into the population inversion curve. In the plot of gain versus frequency of oscillation the superposition of the gain profiles of the individual isotopes gives the resultant gain curve. Thus, in Fig. 4(a), there will be three holes burnt into the resultant gain curve. At the frequency of oscillation, the gain-equals-loss condition will be satisfied by the hole being burnt into the resultant gain curve down to the loss line. As the frequency of oscillation is tuned across the atomic transition, the depths of the holes burnt into the single isotope gain profiles will vary as determined by Eqs. (53) and (54) such as to always maintain the gain-equals-loss condition at the frequency of oscillation in the resultant gain profile. If the gain profile is considered from the point of view of radiation traveling in the opposite direction (same direction as radiation oscillating at ω_1) then the hole burnt into the resultant gain curve will satisfy the gain-equals-loss condition at frequency ω_1. See Fig. 4(b). The image holes will now correspond to the radiation oscillating at frequency ω_2.

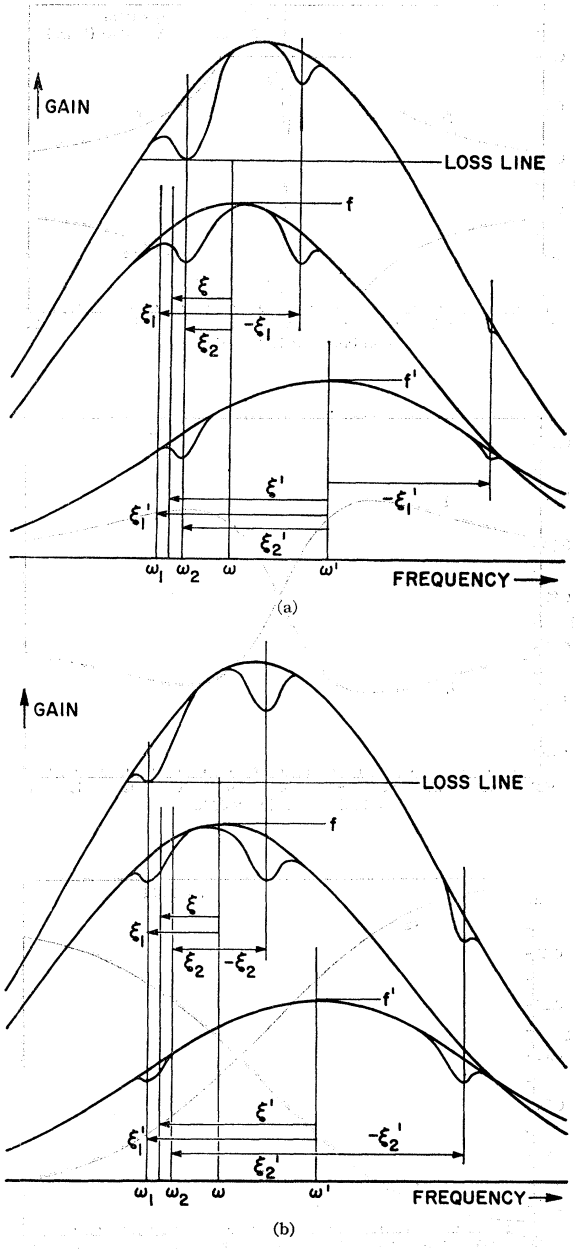

FIG. 4. Figure (a) is the gain profile for a test signal traveling in the same direction as the radiation oscillating at ω_2, for two isotopes having relative concentrations of f and f'. The resultant gain curve is the superposition of the single-isotope gain curves. At ω_2 the resultant gain equals the loss. Figure (b) is the gain profile for a test signal traveling in the same direction as the radiation oscillating at ω_1.

It is interesting to note that the above interpretation of the gain profile as a function of frequency and both the amplitude equations and frequency equations can be obtained using Bennett's[10] "hole burning" model. The width of the holes are taken as twice the natural width and the partial depth only due to the radiation which causes the burning of each hole, is given as the dimensionless intensity multiplied by the gain at the point where the hole is burnt. The total hole burnt into each single isotope curve includes the contribution due to the Lorentzian tail of the image hole.

ACKNOWLEDGMENTS

The author thanks R. J. Collins and J. E. Killpatrick for contributions. The author also thanks J. A. Carruthers, L. A. Baker, and R. E. Var for helpful discussions, and W. E. Lamb, Jr. for helpful comments.

APPENDIX I

From Heer[7], Maxwell's equations on a frame rotating with angular velocity $-\dot{\theta}$ in the direction of the normal to the plane of the cavity, are, for the electric field linearly polarized in the direction of $-\dot{\theta}$,

$$\partial E/\partial z+\partial B/\partial t=0, \tag{I.1}$$

$$\partial H/\partial z+\partial D/\partial t+J=0, \tag{I.2}$$

$$B=\mu_0 H-aE, \tag{I.3}$$

$$D=\epsilon_0 E+P-aH, \tag{I.4}$$

$$J=\sigma E. \tag{I.5}$$

The Poynting vector lies in the z direction and

$$a=2A\dot{\theta}/(Lc^2), \tag{I.6}$$

where L is the optical path of the cavity and A is the

[10] W. R. Bennett, Jr., Phys. Rev. **126**, 580 (1962); *Quantum Electronics—Paris 1963* (Columbia University Press, New York, 1964), p. 441.

geometric area enclosed by L. Maxwell's equations are written only to first order in $\dot{\theta}$. The analogous equation to Eq. (1) is

$$\frac{\partial^2 E}{\partial z^2}-\epsilon_0\mu_0\frac{\omega}{Q}\frac{\partial E}{\partial t}-\epsilon_0\mu_0\frac{\partial^2 E}{\partial t^2}-2a\frac{\partial^2 E}{\partial z\partial t}=-\mu_0\omega^2 P. \quad \text{(I.7)}$$

Expanding the solution of Eq. (I.7) into the set of ECNME, as given by Eq. (4)–(8), and making use of the orthogonality of the ECNME, the equations for the time-dependent ECNME coefficients are found to be

$$\frac{d^2A_n}{dt^2}+\frac{\omega}{Q}\frac{dA_n}{dt}+\Omega_n^2A_n-2aK_n\frac{c^2d\tilde{A}_n}{dt}=\frac{\omega}{\epsilon_0}P_n, \quad \text{(I.8)}$$

$$\frac{d^2\tilde{A}_n}{dt^2}+\frac{\omega}{Q}\frac{dA_n}{dt}+\Omega_n^2\tilde{A}_n+2aK_n\frac{c^2dA}{dt}=\frac{\omega}{\epsilon_0}\tilde{P}_n. \quad \text{(I.9)}$$

For an empty lossless cavity,

$$P_n=\tilde{P}_n=Q^{-1}=0. \quad \text{(I.10)}$$

Expressing A_n and $\tilde{A}_n$ in the form as given by Eqs. (12) and (13) and substituting into Eq. (I.8) and (I.9) subject to Eq. (I.10), it is found upon equating coefficients of $\sin\omega_{1n}t$ and $\cos\omega_{1n}t$ to zero, the equations

$$\omega_{2n}^2-\Omega_n^2-2aK_nc^2\omega_{2n}=0, \quad \text{(I.11)}$$

$$\omega_{1n}^2-\Omega_n^2+2aK_nc^2\omega_{1n}=0. \quad \text{(I.12)}$$

Since

$$\omega^2-\Omega^2=(\omega-\Omega)(\omega+\Omega)\approx 2\omega(\omega-\Omega),$$

Eqs. (I.11) and (I.12) become

$$\omega_{2n}=\Omega_n+aK_nc^2, \quad \text{(I.13)}$$

$$\omega_{1n}=\Omega_n-aK_nc^2. \quad \text{(I.14)}$$

ω_{1n} and ω_{2n} are the empty-cavity normal-mode eigenfunctions Ω_{1n} and Ω_{2n} introduced in Eqs. (17) and (19), respectively. The cavity splitting is

$$\Omega_{2n}-\Omega_{1n}=(2\pi)4A\dot{\theta}/(L\lambda_n). \quad \text{(I.15)}$$

APPENDIX II

Using the single-mode interaction as given by Eq. (30), the first-order Fourier components of the polarization are given by

$$\begin{Bmatrix}P_n^{(1)}(t)\\ \tilde{P}_n^{(1)}(t)\end{Bmatrix}=-\frac{2i|\mu_{ab}|^2}{\hbar L}\int_{-\infty}^{\infty}W(v)dvT(v)\times\int_0^L N(z,t)dz\int_0^\infty d\tau'\exp-(\gamma_{ab}+i\omega)\tau' \quad \text{(II.1)}$$

$$\times\begin{Bmatrix}U_n(z)\\ V_n(z)\end{Bmatrix}[\{E_1\cos((\omega_1+Kv)t'+\Phi_1)+E_2\cos((\omega_2-Kv)t'+\Phi_2)\}U_n(z)$$

$$+\{E_1\sin((\omega_1+Kv)t'+\Phi_1)-E_2\sin((\omega_2-Kv)t\}'+\Phi_2)V_n(z)]+\text{c.c.},$$

where $\tau'=t-t'$ and $W(v)$ is the normalized velocity distribution. $T(v)$ is the proper Lorentz transformation necessary to transform the polarization back to the cavity frame.

Making the rotating wave approximation, Eq. (II.1) becomes

$$\begin{Bmatrix}P_n^{(1)}(t)\\ \tilde{P}_n^{(1)}(t)\end{Bmatrix}=-\frac{i|\mu_{ab}|^2}{\hbar L}\int_{-\infty}^{\infty}W(v)dvT(v)\times\int_0^L N(z,t)dz\int_0^\infty d\tau'\begin{Bmatrix}U_n(z)\\ V_n(z)\end{Bmatrix} \quad \text{(II.2)}$$

$$\times[E_1\exp-(i\omega_1t+i\Phi_1+iKvt+\gamma_{1-}\tau')\times(U_n(z)+iV_n(z))+E_2\exp-(i\omega_2t+i\Phi_2+iKvt+\gamma_{2+}\tau')\times(U_n(z)-iV_n(z))]+\text{c.c.},$$

where

$$\gamma_{i\pm}=\gamma_{ab}+i(\omega-\omega_i\pm Kv). \quad \text{(II.3)}$$

Since $U\pm iV\sim\exp\mp iKz$,
Equation (II.2) is of the form

$$E_1\exp-i(\omega_1t+Kz)+E_2\exp-i(\omega_2t-Kz).$$

Thus $T(v)$ is $\exp iKvt$ and $\exp-iKvt$ for the term in E_1 and E_2, respectively. As a general rule, the Lorentz transformation can be carried out by placing the factor $\exp(\pm iKv)$ next to each bracketed $U\pm iV$.

On writing the bracketed ECNME in exponential form and neglecting second-harmonic spatial terms,[1] Eq. (II.2) becomes

$$P_n^{(1)}(t)=-\frac{i|\mu_{ab}|^2}{\hbar Ku/\pi^{1/2}}\exp[-i(\omega_1t+\Phi_1)]\times\int_{-\infty}^{\infty}dw\exp-w^2\int_0^\infty dx \quad \text{(II.4)}$$

$$\times[E_1\exp(-2\eta x+2i(\xi_1+w)x)+E_2\exp(-i\psi-2\eta x+2i(\xi_2-w)x)]+\text{c.c.},$$

$$\tilde{P}_n^{(1)}(t)=\frac{|\mu_{ab}|^2}{\hbar Ku\pi^{1/2}}\exp[-i(\omega_it+\Phi_1)]\times\int_{-\infty}^{\infty}dw\exp(-w^2)\int_0^\infty dx \quad \text{(II.5)}$$

$$\times[E_1\exp(-2\eta x+2i(\xi_1+w)x)-E_2\exp(-i\psi-2\eta x+2i(\xi_2-w)x)]+\text{c.c.},$$

where the following substitutions have been made:

$$x=\tfrac{1}{2}Ku\tau',\quad \eta=\gamma_{ab}/Ku,\quad \xi_i=(\omega_i-\omega)/Ku,\quad w=v/u.$$

The velocity distribution has been chosen as Maxwellian

$$W(v)dv=(\pi)^{-1/2}\exp(-w^2). \quad \text{(II.6)}$$

Following the technique of Lamb,[1] the first-order coefficients of the Fourier components of the polarization as defined in Eqs. (14) and (15) are found to be

$$S_n^{(1)}(t)=-A[E_1Z_i(\xi_1)+E_2\cos\psi Z_i(\xi_2) -E_2\sin\psi Z_r(\xi_2)], \quad \text{(II.7)}$$

$$C_n^{(1)}(t)=-A[E_1Z_r(\xi_1)+E_2\cos\psi Z_r(\xi_2) +E_2\sin\psi Z_i(\xi_2)], \quad \text{(II.8)}$$

$$\tilde{S}_n^{(1)}=-A[E_1Z_r(\xi_1)-E_2\cos\psi Z_r(\xi_2) -E_2\sin\psi Z_i(\xi_2)], \quad \text{(II.9)}$$

$$\tilde{C}_n^{(1)}=-A[-E_1Z_i(\xi_1)+E_2\cos\psi Z_i(\xi_2) -E_2\sin\psi Z_r(\xi_2)], \quad \text{(II.10)}$$

where the real and imaginary parts of the "plasma dispersion function" are obtained from

$$Z(\xi)=2i\int_0^\infty dx\exp(-x^2-2\eta x+2i\xi x). \quad \text{(II.11)}$$

Substituting Eqs. (II.7)–(II.10) into Eqs. (16)–(19), the self-consistency equations, to first order, are found to be

$$\dot{E}_j+\tfrac{1}{2}(\omega/Q_j)E_j=\tfrac{1}{2}(\omega/\epsilon_0)AE_jZ_i(\xi_j)\ j=1,2, \quad \text{(II.12)}$$

$$(\Omega_j-\omega_j-\dot{\Phi}_j)E_j=-\tfrac{1}{2}(\omega/\epsilon_0)AE_jZ_r(\xi_j)\ j=1,2. \quad \text{(II.13)}$$

For the Doppler width much larger than the natural width ($\eta\ll1$), the expansion of Eq. (II.11) gives

$$Z_i(\xi)=\pi^{1/2}\exp(-\xi^2)-2\eta[1-2\xi F(\xi)]+\cdots, \quad \text{(II.14)}$$

$$Z_r(\xi)=-2F(\xi)+2\pi^{1/2}\xi\eta\exp(-\xi^2)+\cdots, \quad \text{(II.15)}$$

with $F(\xi)$ given by Eq. (33).

Equations (31) and (32) are obtained from Eqs. (II.12 and (II.13) for $\Phi=\eta=0$.

APPENDIX III

The second-order population-inversion density is given as

$$\Delta\rho^{(2)}(z,v,t)=T(v)\Delta\rho^{(0)}(z,v,t)\int_0^\infty d\tau'\int_0^\infty d\tau'' \times[\exp(-\gamma_a\tau')+\exp(-\gamma_b\tau')] \times\exp[-(\gamma_{ab}+i\omega)\tau''] \times V_{ba}(t')V_{ab}(t'')+\text{c.c.}, \quad \text{(III.1)}$$

where the substitutions $\tau'=t-t'$, $\tau''=t'-t''$, have been made and the interaction is given by Eq. (30). The zeroth-order population-inversion density (inversion in the absence of stimulated emission) is given by

$$\Delta\rho^{(0)}(z,v,t)=W(v)N(z,t). \quad \text{(III.2)}$$

Making use of the rotating-wave approximation, only the positive and negative frequency components of $V_{ba}(t')$ and $V_{ab}(t'')$, respectively, give contributions. The interaction terms then have the form

$$V_{ba}(t')\sim E_1\exp[i(\omega_1+Kv)t'+\Phi_1](U-iV) +E_2\exp[i(\omega_2-Kv)t'+\Phi_2](U+iV), \quad \text{(III.3)}$$

$$V_{ab}(t'')\sim E_1\exp[-i(\omega_1+Kv)t''-\Phi_1](U+iV) +E_2\exp[-i(\omega_2-Kv)t''-\Phi_2] \times(U-iV). \quad \text{(III.4)}$$

The cross terms in E_1E_2 have the factor $(U\pm iV)^2\sim\exp\mp2iKz$ and can be neglected. The interaction terms are then of the form

$$V_{ba}(t')V_{ab}(t'')\sim[E_1^2\exp i(\omega_1+Kv)\tau'' +E_2^2\exp i(\omega_2-Kv)\tau''] \times(U+iV)e^{iKvt}(U-iV)e^{-iKvt}. \quad \text{(III.5)}$$

In Eq. (III.5) the Lorentz transformation has been carried out by the rule stated in Appendix II.

The double integral on Eq. (III.1) can now be evaluated to give

$$\Delta\rho^{(2)}(z,v,t)=-\eta\Delta\rho^{(0)}(z,v,t)[I_1[\eta-i(\xi_1+w)]^{-1} +I_2[\eta-i(\xi_2-w)]^{-1}]+\text{c.c.} \quad \text{(III.6)}$$

Combining the complex conjugate term and averaging over the cavity length results in Eq. (36).

APPENDIX IV

The third-order Fourier components of the polarization are given by

$$\begin{Bmatrix}P_n^{(3)}(t)\\ \tilde{P}_n^{(3)}(t)\end{Bmatrix}=-\frac{2i|\mu_{ba}|}{L}\int_0^\infty W(v)T(v)dv\int_0^L N(z,t)dz \times\int_0^\infty d\tau'\int_0^\infty d\tau''\int_0^\infty d\tau''' \times\exp[-(\gamma_{ab}+i\omega)\tau'] \times[\exp(-\gamma_a\tau'')+\exp(-\gamma_b\tau'')] \times\{\exp[-(\gamma_{ab}+i\omega)\tau''']+\text{c.c.}\} \times\begin{Bmatrix}U_n(z)\\ V_n(z)\end{Bmatrix}V_{ab}(t')V_{ba}(t'') \times V_{ab}(t''')+\text{c.c.}, \quad \text{(IV.1)}$$

where the substitutions

$$\tau'=t-t', \quad \tau''=t'-t'', \quad \tau'''=t''-t''' \quad \text{(IV.2)}$$

have been made and the interaction is given by Eq. (30).

In making the rotating-wave approximation, only the negative, positive, and negative frequency components of $V_{ab}(t')$, $V_{ba}(t'')$, and $V_{ab}(t''')$, respectively, give contributions to the term in $\exp-(\gamma_{ab}\pm i\omega)\tau'''$.

Each interaction term then contains factors of the form $(U\pm iV)$. The Lorentz transformation is carried out

by following the role in inserting the factor $\exp(\pm iKv)$ next to each $(U\pm iV)$. Making use of Eq. (IV.2), the integrand of Eq. (IV.1) becomes

$$\frac{i|\mu|^4}{8\hbar^3 L}\begin{Bmatrix}U\\V\end{Bmatrix}\exp[-i(\omega_1 t+\Phi_1)]$$
$$\times[\exp(-\gamma_a\tau'')+\exp(-\gamma_b\tau'')]$$
$$\times\{E_1(U+iV)\exp(-\gamma_{1-}\tau')$$
$$+E_2(U-iV)\exp[-i(\psi+\gamma_{2+}\tau')]\}$$
$$\times(E_1^2\exp(-\gamma_{1-}\tau''')+E_2^2\exp(-\gamma_{2+}\tau''')$$
$$+E_1E_2(U-iV)^2\exp\{-[\gamma_1\tau'''$$
$$+iKv(2\tau'+2\tau''+\tau''')+i\psi-i(\omega_2-\omega_1)$$
$$\times(\tau'+\tau''+\tau''')]\}+E_1E_2(U+iV)^2$$
$$\times\exp\{-[\gamma_2\tau'''-iKv(2\tau'+2\tau''+\tau''')$$
$$-i\psi+i(\omega_2-\omega_1)(\tau'+\tau''+\tau''')]\}$$
$$+\text{c.c.})+\text{c.c.}, \quad \text{(IV.3)}$$

where

$$\gamma_i=\gamma_{ab}+i(\omega-\omega_i),$$
$$\gamma_{i\pm}=\gamma_{ab}+i(\omega-\omega_i\pm Kv),$$
$$\psi=(\omega_2-\omega_1)t+\Phi_2-\Phi_1.$$

The integration over the cavity length can now be performed, neglecting second and fourth harmonics of $\exp(\pm iKz)$. After performing the velocity integration, the resulting integral can be simplified for the case of the "Doppler limit," i.e., the Doppler width Ku being much larger than the natural width γ_{ab}. By making the delta-function approximation[1] the portion giving the dominent contribution can be picked out as

$$P_n^{(3)}(t)=\frac{i|\mu|^4\bar{N}(t)\gamma_{ab}}{\hbar^3\gamma_a\gamma_b(Ku)^2}\exp[-(\omega_1 t+\Phi_1)]$$
$$\times\int_0^\infty dx\int_0^\infty dy\exp\{-[2\eta(x+y)+(x-y)^2]\}$$
$$\times\{E_1^3\exp[+2i\xi_1(x-y)]$$
$$+E_2^3\exp[-i\psi+2i\xi_2(x-y)]$$
$$+E_1E_2^2\exp[2i(\xi_1 x+\xi_2 y)]$$
$$+E_1^2E_2\exp[-i\psi+2i(\xi_2 x+\xi_1 y)]\}$$
$$+\text{c.c.}, \quad \text{(IV.4)}$$

where the integration over τ'' has been performed and the substitutions as introduced in Appendix II have been made. Rather than actually evaluating Eq. (IV.4) with the delta-function approximation, use of the integral

$$\int_0^\infty\int_0^\infty dxdy\exp[2i(\xi_a x+\xi_b y)-2\eta(x+y)-(x-y)^2]$$
$$=\frac{\eta+i\xi}{8i\eta^2}\mathfrak{L}(\xi)[Z(\xi_a)+Z(\xi_b)], \quad \text{(IV.5)}$$

where $\xi=\frac{1}{2}(\xi_a+\xi_b)$ and $Z(\xi)$ being the plasma dispersion function, will enable the exact evaluation of Eq. (IV.4).

The integral in Eq. (IV.5) has been evaluated by use of the substitution $\alpha=x+y$, $\beta=x-y$, and

$$\int_0^\infty\int_0^\infty dxdy\rightarrow\int_0^\infty d\beta\int_\beta^\infty d\alpha \text{ (integrand even in } \beta).$$

The coefficients of the Fourier components of the polarization for Eq. (IV.4) are then obtained as

$$S_n^{(3)}(t)=A\{E_1I_1Z_i(\xi_1)+E_2I_2\cos\psi Z_i(\xi_2)$$
$$+E_1I_2\mathfrak{L}(\xi)[\bar{Z}_i+(\xi/\eta)\bar{Z}_r]$$
$$+E_2I_1\mathfrak{L}(\xi)[(\cos\psi+(\xi/\eta)\sin\psi)\bar{Z}_i$$
$$-(\sin\psi-(\xi/\eta)\cos\psi)\bar{Z}_r]\}, \quad \text{(IV.6)}$$

$$C_n^{(3)}(t)=A\{E_2I_2\sin\psi Z_i(\xi_2)$$
$$+E_1I_2\mathfrak{L}(\xi)[\bar{Z}_r-(\xi/\eta)\bar{Z}_i]$$
$$+E_2I_1\mathfrak{L}(\xi)[(\sin\psi-(\xi/\eta)\cos\psi)\bar{Z}_i$$
$$+(\cos\psi+(\xi/\eta)\sin\psi)\bar{Z}_r]\}, \quad \text{(IV.7)}$$

with $\xi=\frac{1}{2}(\xi_1+\xi_2)$, $\bar{Z}=\frac{1}{2}[Z(\xi_1)+Z(\xi_2)]$. In like manner it is found that

$$\tilde{P}_n^{(3)}(t)=iP_n^{(3)}(t)\ [\text{terms with } \exp(-\psi)$$
$$\text{are multiplied by minus one}],$$

and hence

$$\tilde{C}_n^{(3)}(t)=S_n^{(3)}(t)\ (\text{terms without } \psi$$
$$\text{are multiplied by minus one}), \quad \text{(IV.8)}$$

$$\tilde{S}_n^{(3)}(t)=C_n^{(3)}(t)\ (\text{terms with } \psi$$
$$\text{are multiplied by minus one}). \quad \text{(IV.9)}$$

Using Eqs. (16)–(19) and Eqs. (IV.6)–(IV.9), the self-consistant equations, with only the dominent third-order contribution, are found to be

$$\dot{E}_1+\tfrac{1}{2}(\omega/Q)E_1=\tfrac{1}{2}(\omega/\epsilon_0)AE_1$$
$$\times\{Z_i(\xi_1)-I_1Z_i(\xi_1)-I_2\mathfrak{L}(\xi)$$
$$\times[\bar{Z}_i+(\xi/\eta)\bar{Z}_r]\}, \quad \text{(IV.10)}$$

$$\dot{E}_2+\tfrac{1}{2}(\omega/Q)E_2=\tfrac{1}{2}(\omega/\epsilon_0)AE_2$$
$$\times\{Z_i(\xi_2)-I_2Z_i(\xi_2)-I_1\mathfrak{L}(\xi)$$
$$\times[\bar{Z}_i+(\xi/\eta)\bar{Z}_r]\}, \quad \text{(IV.11)}$$

$$(\omega_1+\dot{\Phi}_1-\Omega_1)=\tfrac{1}{2}(\omega/\epsilon_0)A\{Z_r(\xi_1)+I_2\mathfrak{L}(\xi)$$
$$\times[(\xi/\eta)\bar{Z}_i-\bar{Z}_r]\}, \quad \text{(IV.12)}$$

$$(\omega_2-\dot{\Phi}_2-\Omega_2)=\tfrac{1}{2}(\omega/\epsilon_0)A\{Z_r(\xi_1)+I_1\mathfrak{L}(\xi)$$
$$\times[(\xi/\eta)\bar{Z}_i-\bar{Z}_r]\}. \quad \text{(IV.13)}$$

If the delta function approximation were made, Eqs. (IV.10) and (IV.12) would read, respectively,

$$\dot{E}_1+\tfrac{1}{2}(\omega/Q)E_1=\tfrac{1}{2}(\omega/\epsilon_0)AE_1 \times[Z_i(\xi_1)-(\pi^{1/2})I_1-(\pi^{1/2})I_2\mathfrak{L}(\xi)], \quad \text{(IV.14)}$$

$$(\omega_1+\Phi_1-\Omega_1)=\tfrac{1}{2}(\omega/\epsilon_0)A \times[Z_r(\xi_1)+(\pi^{1/2})I_2\mathfrak{L}(\xi)(\xi/\eta)]. \quad \text{(IV.15)}$$

Now consider one of the neglected contributions to the polarization, having the form of Eq. (IV.4) with $y\rightarrow -y$ in all the exponentials except $\exp-2\eta(x+y)$. Using the integral

$$\int_0^\infty\int_0^\infty dxdy\,\exp[2i(\xi_a x+\xi_b y)-2\eta(x+y)-(x+y)^2] =(8\Delta\xi)^{-1}[Z(\xi_a)-Z(\xi_b)], \quad \text{(IV.16)}$$

where $\Delta\xi=\frac{1}{2}(\xi_b-\xi_a)$, the right-hand sides of Eqs. (IV.10) and (IV.11), respectively, take the form,

$$Z_i(\xi_1)-I_1Z_i(\xi_1)-I_2\mathfrak{L}(\xi)[\bar{Z}_i-(\eta/\xi)\bar{Z}_r] -2\eta I_1[1-\eta Z_i(\xi_1)+\xi_1 Z_r(\xi_1)], \quad \text{(IV.17)}$$

$$Z_r(\xi_1)+(\xi/\eta)I_2\mathfrak{L}(\xi)\{\bar{Z}_i-(\eta/\xi)\bar{Z}_r -\tfrac{1}{2}[1+(\eta/\xi)^2][Z_i(\xi_1)-Z_i(\xi_2)]\} +2\eta I_1[\xi_1 Z_i(\xi_1)+\eta Z_r(\xi_2)], \quad \text{(IV.18)}$$

where use has been made of the identity

$$(\eta/\xi)-(\xi/\eta)\mathfrak{L}(\xi)=(\eta/\xi)\mathfrak{L}(\xi).$$

Thus the effect of not making the delta-function approximation is to introduce additional terms of the order of $\eta\ll 1$. Neglecting these terms is equivalent to neglecting the effects of natural broadening on the lineshape for the third-order polarization. Equations (42)–(46) are written in this approximation and for the case of small rotations ($\Delta\xi\ll\eta$).

Note added in proof. It has been brought to my attention that an adaptation of Lamb's model to the traveling-wave case has been presented by C. V. Heer in a report at the 1964 Symposium on Unconventional Inertial Sensors, Polytechnic Institute of Brooklyn Graduate Center, Farmingdale, New York (unpublished).

PHYSICAL REVIEW VOLUME 139, NUMBER 3A 2 AUGUST 1965

Index of Refraction and Sum Rules for Helium*

R. MIGNERON† AND J. S. LEVINGER‡
Cornell University, Ithaca, New York

(Received 12 November 1964; revised manuscript received 23 March 1965)

Recent measurements by Lowry and by Lukirskii of the atomic photoeffect for helium can be combined with calculations for discrete transitions and for the high-energy photoeffect to give the oscillator density for the entire range. We use dispersion theory to calculate the index of refraction n. We find satisfactory agreement with experiments in the visible and in the near ultraviolet, and we predict the value of n from 2700 to 600 Å. Our predicted values agree satisfactorily with values calculated by Chen and Dalgarno. We use these oscillator densities to calculate the sum rules $S(0)$, $S(1)$, and $S(2)$, which weight with the zeroth, first, and second powers of the photon energy, respectively. Each result agrees with values based on ground-state wave functions to 5% accuracy. We conclude that in general the oscillator density is now known to about 5% accuracy.

I. INTRODUCTION

LOWRY *et al.*[1] have recently measured the absorption cross section for helium for photons in the energy range from the photoeffect threshold of 1.807 to 8.82 Ry; while Lukirskii *et al.*[2] have worked up to energies of 20.6 Ry. We are interested in dispersion-theoretic calculations of the index of refraction n, and also in calculations of oscillator-strength sum rules $S(p)$ weighted with the pth power of the photon energy. For our calculations we need both the oscillator strengths for discrete transitions, and we need the oscillator density at all energies. We use Schiff and Pekeris' calculations[3] for discrete transitions, calculations by Stewart and Webb[4] from 20.6 to 130 Ry, and calculations by Salpeter and Zaidi.[5] We have chosen the Stewart-Webb calculation for the velocity matrix element with Hartree-Fock wave functions. We add to this the cross section for double excitation calculated by Salpeter and Zaidi. There is a 10% discrepancy

* Supported in part by the U. S. Office of Naval Research.
† Canadian Commonwealth Fellow, now at Imperial College, University of London. This paper is based in part on an M.S. thesis, Cornell University, 1964 (unpublished).
‡ AVCO Visiting Professor, now at Rensselaer Polytechnic Institute.
[1] J. F. Lowry, D. L. Ederer, and D. H. Tomboulian, Phys. Rev. 137, A1054 (1965).
[2] A. P. Lukirskii, I. A. Brytov, and T. M. Zimkina, Opt. i Spektroskopiya 17, 438 (1964) [English transl.: Opt. Spectry. (USSR) 17, 234 (1964).
[3] B. Schiff and C. L. Pekeris, Phys. Rev. 134, A638 (1964).
[4] A. L. Stewart and T. G. Webb, Proc. Phys. Soc. (London) 82, 532 (1963).
[5] E. E. Salpeter and M. H. Zaidi, Phys. Rev. 125, 248 (1962).